Mon. Not. R. astr. Soc. (1974) **166,** 355–371.

THE SPECTRUM OF THE GALACTIC NON-THERMAL BACKGROUND RADIATION—II

Observations at 408, 610 and 1407 MHz

A. S. Webster

(Communicated by John Shakeshaft)

(Received 1973 August 13)

SUMMARY

Between 408, 610 and 1407 MHz the mean differential temperature spectral index of the galactic non-thermal radiation is found to be close to 2·80, although the exact value varies with direction. Several regions with anomalous spectra are associated with previously-known features of the continuum background.

1. INTRODUCTION

Paper I (Sironi 1974) described measurements of the differential temperature spectrum of the galactic background radiation by means of scaled arrays at 151·5 and 408 MHz. This paper describes related observations using pyramidal horn antennas at 408, 610 and 1407 MHz. The particular objectives were twofold: first to investigate how closely the differential spectral index at these frequencies has approached its high-frequency asymptotic value of $\beta \approx 2{\cdot}8$–$2{\cdot}9$ (Penzias & Wilson 1966; Altenhoff 1968; Conklin 1970), and second to search for possible variations of spectrum with direction, on all angular scales greater than the beamwidth of $15° \times 15°$.

The measurements were difficult for several reasons. One is that 408 and 610 MHz are frequencies so close together that extreme care is necessary if meaningful spectral data are to be determined. For example, an error of only 4 per cent in the scale of the antenna temperatures of either system would result in an error of 0·1 in the value of the spectral index. Another is that by 1407 MHz the brightness temperature of the galactic non-thermal radiation at high latitudes has dropped to values of 1 K and less, so very small changes of antenna temperature have to be measured in the face of such diurnal effects as the variation of ambient temperature and mains voltage. Special methods of overcoming these problems were devised.

Section 2 describes the receiving systems, Section 3 the results and Section 4 the derivation of spectral indices. The conclusions are summarized in Section 5.

2. THE RECEIVING SYSTEMS

2.1 *The antennas*

For a background survey at high frequency a horn antenna has a substantial advantage over an array of dipoles in that (i) the side lobes are considerably lower than those of a comparable array, thereby reducing the contribution from extraneous sources, (ii) the beam pattern is better defined, and (iii) the antenna loss is much

smaller and more readily calculated. Scaled horns as described by Howell (1970) were therefore used. These were of copper sheet at 408 and 610 MHz and of aluminium sheet at 1407 MHz. The 15° beamwidths were sufficiently small that spectral variations over the sky could be investigated but sufficiently large that, first, the background radiation swamped the contributions of all but the most powerful discrete sources and, second, the net polarization in most directions is low enough that little error is introduced by using antennas which respond only to one linearly polarized component of the total flux.

The horns were mounted with their *E*-planes coincident with the local meridional plane and could be tipped to different declinations. The input probes were matched to 50 Ohm impedance with VSWRs of 1·05 or less across the bandwidths of 4 MHz.

2.2 *The receivers*

The receivers were basically Dicke switching radiometers. Because of the variation of input temperature with frequency, the designs of the front ends differed from system to system and are described separately, but beyond the Dicke switches the receivers were essentially identical. Transistor amplifiers provided the first stages of gain and gave system noise temperatures of about 500 K. The final outputs were smoothed with RC time constants of 8 s and recorded on paper charts.

2.2.1 *The* 408 *and* 610 *MHz systems.* These (Fig. 1) compared the antenna temperature with the 77 K noise temperature of a resistor immersed in liquid nitrogen (the cold load CL2). The liquid nitrogen loads were designed (Webster 1972) to provide a steady reference temperature despite variations of liquid nitrogen level in the Dewars. The main cause of changes in the reference temperature was then the dependence of boiling temperature on atmospheric pressure; 0·086 K for the typical daily range of 100 millibars.

Ideally the reference temperatures would have been nearer the expected antenna temperatures of about 25 K and 10 K, respectively, but the convenience of liquid nitrogen was an important consideration and approximate balance was achieved by injecting noise from a noise diode via a directional coupler. This noise diode also functioned as the transfer standard for calibrating the scale of antenna temperature. At regular intervals when observing, the current through the noise diode was increased by a known amount with a consequent change of receiver output. This change of output was calibrated against the thermodynamic scale of temperature in a separate experiment.

At first, trouble was experienced from a small diurnal variation of the zero-level of the system. This problem was overcome by including the switch S1 and the cold load CL1 in order to be able to measure the zero level from time to time whilst observing. S1 was a well-matched electromechanical switch with very low loss. It was connected directly onto the antenna termination and by only 200 mm of cable to the cold load CL1. By minimizing the lengths of cable before the switch, with their unavoidable loss, the changes in output zero-level due to differential changes in the temperature of the cables were reduced to an acceptable amount.

An automatic programming device controlled the times of observation, calibration and zero-level determination as shown in Table I, where I_0 is the current through the noise diode which approximately equalized the noise powers at the terminals of the Dicke switch and I_1 is a greater current which increased the noise

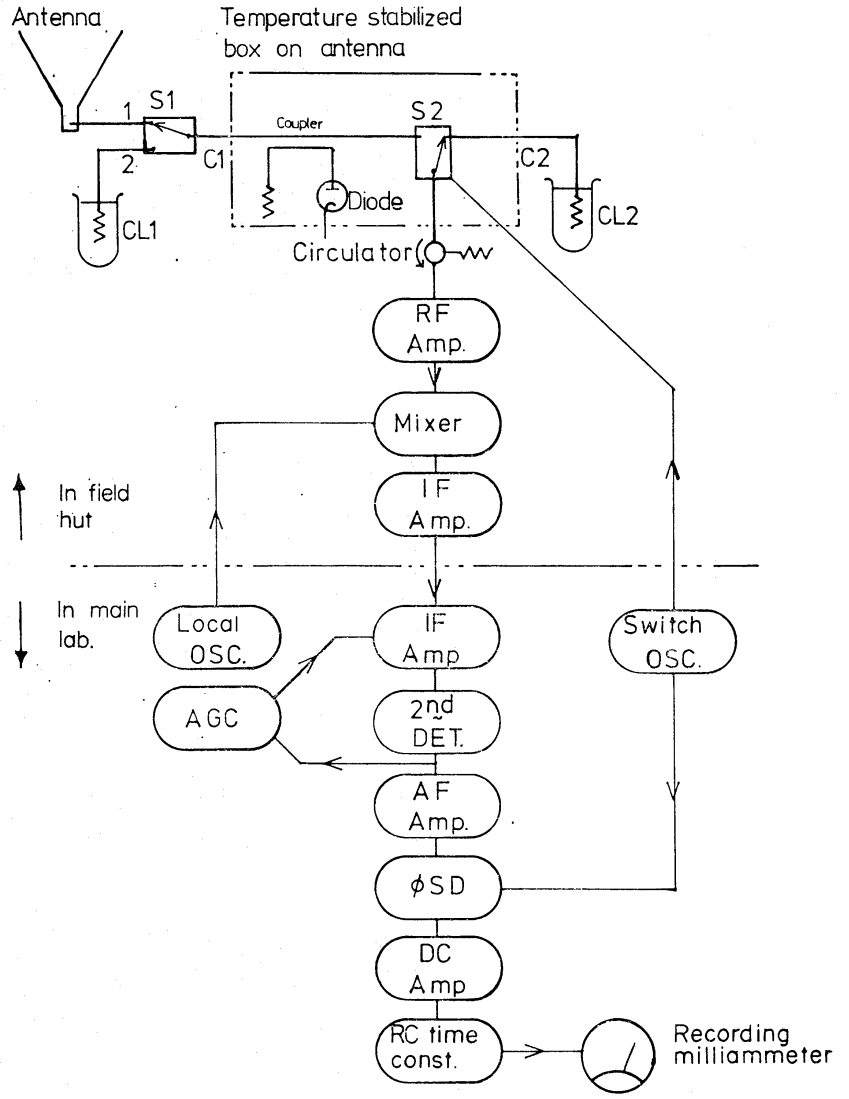

FIG. 1. *A block diagram of the* 408 *and* 610 *MHz receiving systems. S, switch; C, cable; CL, cold load.*

contribution through the directional coupler by about 30 K at 408 MHz and 10 K at 610 MHz. The 32-min cycle was divided into four phases of equal length. In phases 1 and 3 observations were made, in phase 2 the gain was calibrated and in phase 4 the zero-level was determined.

TABLE I

The automatic sequence of operations employed when observing with the 408 *and* 610 *MHz systems*

Phase	1	2	3	4
Noise diode current (mA)	I_0	I_1	I_0	0
Position of switch S1	1	1	1	2

2.2.2 *The* 1407 *MHz system.* At 1407 MHz the antenna temperature is about 5 K, indicating the need for a reference load in liquid helium. None was available with sufficient long-term stability and it was decided to use instead a second

antenna directed at the celestial north pole as the reference. Even with this arrangement it was plain from the outset that special precautions would be necessary against the effects of changes in temperature of the receiver and cables, and variations of match of the horns which would alter the amount of noise from the receiver reflected back into the system. The method adopted was to make the second antenna identical with the first and to mount them both on a turntable so that the directions in which they pointed could be interchanged. Each antenna was thus alternately the observing antenna and the reference, and any instrumental error signal due to differential losses and mismatches could be made to cancel out. The

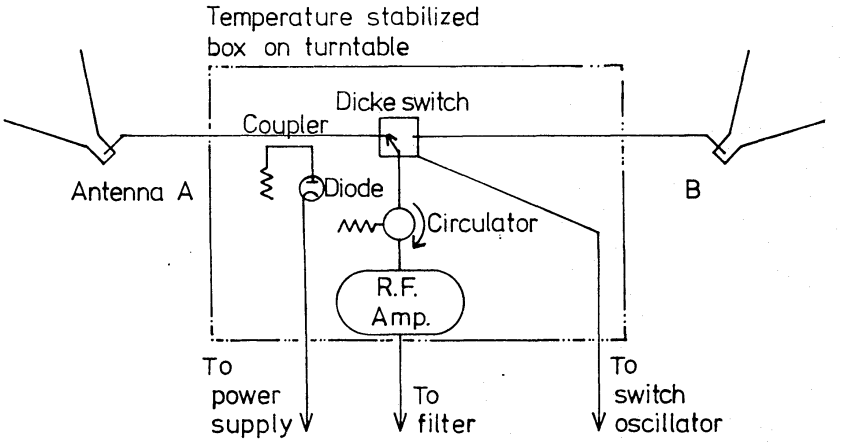

FIG. 2. *A block diagram of the radio frequency head of the 1407 MHz system.*

front end of this receiver was also mounted on the turntable and is outlined in Fig. 2. Since the antenna temperatures were approximately equal, the noise diode was used only for calibration and not for offsetting. The turntable stood inside an enclosure of aluminium sheet, open only to the sky, to eliminate the possible effects of ground radiation. The automatic programming device also controlled this experiment, interchanging the directions of the horns every 10 min and operating the noise diode for 5 min in every hour to provide a calibration signal of about 5 K.

2.3 *Calibration*

2.3.1 *The 408 and 610 MHz systems.* Because of the comparatively small fractional change of frequency between 408 and 610 MHz, it was necessary to calibrate the scales of antenna temperature very accurately if the spectral index derived was to be meaningful. Advantage was taken of the fact that the gradient of a T–T plot is a dimensionless quantity so the scales along the two axes need only be known relatively and not absolutely. The 408 and 610 MHz systems were calibrated against the same noise temperature difference, which eliminated the need to measure any temperatures at all and thus eliminated possible errors from thermometry. The standards of noise temperature were two matched loads, one immersed in melting ice and the other in water maintained to within 0·1 K of a temperature near 40 °C by a thermistor, electrical heater and feedback amplifier.

The procedure employed when calibrating the 408 MHz system was as follows. The antenna was disconnected and the 40 °C load connected directly to port 1 of switch S1 (Fig. 1). CL1 was disconnected and the load in melting ice connected

to port 2 by a very short cable. CL2 was also disconnected and replaced by a load in a vacuum flask of water at about 80°C; the purpose of this was to calibrate the system at balance with the necessary offset from the noise diode and coupler approximately equal to the offset chosen when observing (i.e. with the noise diode current roughly equal to I_0).

First the switch S1 was set to port 2 and the noise diode current adjusted until the Dicke system was balanced. Then port 1 was selected and the system balanced again. Finally the system was rebalanced with the switch at port 2, to compensate for the slow cooling of the load in water at 80°C which was not stabilized.

The same procedure was followed for the 610 MHz system, using the same calibrating apparatus. For each system the difference in the average noise diode currents when the switches S1 were at ports 1 and 2 corresponded to the difference in thermodynamic temperature between the baths at 0°C and 40°C, less a very small amount caused by attenuation in the coaxial cables connecting the resistors in the loads to the switch. This attenuation was measured to be 0·06 dB at 408 MHz and, because the attenuation scales as the square root of the frequency, the change of the calibrating signal was only about 0·1 per cent between 408 and 610 MHz which was negligible.

For comparison with surveys calibrated by a different method, such as the present 1407 MHz survey, the difference in temperature between the baths, corrected for cable losses, had to be known absolutely. The water temperatures were measured by a mercury-in-glass thermometer good to 0·1 K and the difference in temperatures multiplied by 0·995 to allow for the attenuation.

Both systems were calibrated six times during the observing period. The temperature scale appropriate to any day's drift scan was taken as the mean of the two calibrations closest in time to that day.

2.3.2 *The 1407 MHz system.* The gain of this system was set so high that the 40 K difference between the loads used to calibrate the 408 and 610 MHz systems drove it well off scale. The system had therefore to be calibrated independently, by replacing the antennas by loads in water baths, changing the temperature of one of the baths by about 10 K and noting the change in noise diode current necessary to keep the system in balance.

3. RESULTS

At 408 and 610 MHz the antenna and atmospheric losses were so small that the antenna temperatures needed no correction to convert them into mean sky brightness temperatures. The sky brightness temperatures measured at these frequencies over a range of right ascension (RA) at declinations $\delta = 0°$, $+16°$, $+40°$, $+50°$, and $+65°$ are listed in Table II. At 408 MHz an average of 10 days' observations was combined at each declination, and never fewer than 7. At 610 MHz these numbers were 9 and 5 respectively, owing to the greater susceptibility of the antenna impedance to wet weather. The scatter of the measurements from day to day gave the following rms values for the errors in the average brightness temperatures listed in Table II at 408 and 610 MHz: 0·06 and 0·04 K at all declinations except $\delta = 0°$, where the errors were 0·09 and 0·06 K respectively.

The 1407 MHz system was even more susceptible to the weather and many other factors besides, so useful results were only obtained at declinations $+16°$ and $+40°$. At $\delta = +16°$, 8 days' observations were averaged, and at $+40°$,

TABLE II

The measured mean sky brightness temperatures, in units of degrees K

RA	$\delta = 00°$		$\delta = +16°$			$\delta = +40°$			$\delta = +50°$		$\delta = +65°$	
h m	T_{408}	T_{610}	T_{408}	T_{610}	T_{1407}	T_{408}	T_{610}	T_{1407}	T_{408}	T_{610}	T_{408}	T_{610}
00 00	—	—	—	—	—	17·5	7·51	1·01	22·8	11·89	34·6	11·83
00 12												
00 24	—	—	—	—	—	17·4	6·93	1·05	21·8	—	33·4	11·53
00 36												
00 48	—	—	—	—	—	17·5	6·64	1·04	21·2	—	—	—
01 00												
01 12	—	—	—	—	—	17·9	6·99	1·06	21·0	—	—	—
01 24												
01 36	—	—	—	—	—	18·3	—	1·11	21·1	—	—	—
01 48												
02 00	—	—	—	—	—	18·9	—	1·12	21·8	—	—	—
etc.												
	—	—	—	—	—	19·7	—	1·15	22·9	—	—	—
	—	—	—	—	—	20·6	—	—	24·0	—	—	—
03 00												
	—	—	—	—	—	21·3	—	—	24·8	—	—	—
	—	—	—	—	—	22·2	8·71	—	25·4	—	—	—
04 00	—	—	—	—	—	23·0	9·06	—	25·4	—	—	—
	—	—	—	—	—	24·3	9·18	—	24·4	—	—	—
	—	—	—	—	—	24·8	9·18	—	23·3	10·79	—	—
05 00	9·6	4·01										
	10·8	4·25	—	—	—	24·9	8·82	—	22·0	10·06	—	—
	12·5	4·56										
	13·6	5·30	—	—	—	23·4	8·35	—	20·4	9·26	—	4·97
	14·9	5·55										
06 00	16·0	5·86	—	—	—	21·5	7·63	—	17·5	8·49	—	4·50
	16·8	6·04										
	17·2	5·98	19·5	—	0·69	19·1	6·91	—	15·8	7·75	—	4·02
	17·3	5·86										
	16·8	5·67	18·4	6·45	0·62	16·6	5·65	—	13·8	7·09	—	3·55
07 00	15·7	5·05										
	14·2	4·38	14·3	5·25	0·52	14·5	5·36	—	11·9	6·48	—	3·08
	11·9	3·70										
	10·5	3·14	10·8	4·12	0·30	12·0	4·65	—	9·9	5·87	6·5	2·54
	8·8	2·53										
08 00	7·3	2·22	7·4	2·98	0·24	9·5	3·99	—	8·1	5·39	5·6	2·25
	5·6	1·66										
	4·4	1·42	4·7	2·27	0·16	7·2	3·38	—	6·2	4·91	4·8	1·95
	3·2	1·05										
	2·7	0·80	2·6	1·55	0·13	5·3	3·04	—	4·7	4·42	4·1	1·60
09 00	1·9	0·49										
	1·6	0·43	1·4	1·19	0·16	4·2	2·71	—	3·4	4·12	3·5	1·42
	1·4	0·55										
	1·4	0·37	1·3	1·02	0·12	3·7	2·36	—	2·4	3·82	3·1	1·30
	1·6	0·49										
10 00	1·4	0·55	1·6	1·13	0·11	3·7	2·24	—	2·0	3·58	2·6	1·12
	1·8	0·62										

TABLE II—*continued*

RA h m	δ = 00°		δ = +16°			δ = +40°			δ = +50°		δ = +65°	
	T_{408}	T_{610}	T_{408}	T_{610}	T_{1407}	T_{408}	T_{610}	T_{1407}	T_{408}	T_{610}	T_{408}	T_{610}
	2·2	0·74	2·0	1·25	0·17	3·8	2·12	—	2·0	3·46	2·2	1·06
	2·5	0·80										
	2·7	0·92	2·5	1·43	0·22	4·1	2·21	—	2·0	3·39	1·8	1·01
11 00	3·1	1·05										
	3·5	1·23	3·0	1·67	0·20	4·7	2·38	—	2·4	3·52	1·8	1·01
	4·0	1·36										
	4·5	1·48	4·1	1·91	0·25	5·4	2·65	—	3·0	3·52	1·8	0·95
	5·2	1·79										
12 00	6·1	2·16	5·0	2·27	0·25	5·9	2·65	—	3·1	3·52	1·8	0·95
	7·1	2·28										
	8·3	2·65	6·2	2·81	0·38	6·2	2·77	—	3·2	3·52	1·8	1·01
	9·4	2·96										
	10·1	2·96	7·6	3·34	0·40	6·5	2·77	—	3·4	3·52	1·8	1·06
13 00	10·5	3·14										
	10·6	3·39	9·3	3·82	0·44	6·5	2·88	0·55	3·5	3·52	1·8	1·06
	10·4	3·33										
	10·6	3·46	11·0	4·30	0·55	6·8	3·07	0·60	3·6	3·52	1·8	1·12
	10·8	3·58										
14 00	10·9	3·76	12·9	4·78	0·57	7·5	3·24	0·57	4·0	3·64	2·1	1·18
	11·7	4·13										
	12·5	4·37	15·0	5·37	0·62	8·3	3·32	0·58	4·4	3·76	2·4	1·24
	13·6	4·81										
	14·8	4·93	17·6	5·97	0·67	9·2	3·57	0·59	5·0	4·00	3·0	1·30
15 00	15·9	5·43										
	16·8	5·80	20·2	6·69	0·75	10·0	3·69	0·58	5·6	4·18	3·7	1·54
	17·7	6·05										
	18·6	6·60	22·8	7·40	0·74	10·9	3·92	0·63	6·2	4·36	4·4	1·77
	19·9	6·90										
16 00	21·0	7·52	25·2	8·12	0·80	11·8	4·25	0·60	7·1	4·66	5·2	2·01
	23·0	8·02										
	25·4	8·81	28·1	8·96	0·88	12·9	4·57	0·63	7·9	4·96	6·0	2·19
	27·9	9·93										
	32·4	11·21	30·8	9·73	1·01	13·8	4·93	0·63	8·9	5·34	6·9	2·43
17 00	37·4	12·76										
	41·8	14·30	33·6	10·62	1·14	15·0	5·39	0·66	10·6	5·70	7·9	2·72
	49·9	16·58										
	58·2	19·36	37·3	11·94	1·29	16·6	6·10	0·70	11·9	6·30	9·0	3·19
	67·5	21·70										
18 00	—	—	42·5	14·33	1·52	19·0	6·93	0·81	14·5	7·09	10·2	3·67
	—	—	52·6	16·83	1·98	22·9	8·49	0·95	17·3	8·12	11·5	4·32
	—	—	64·1	19·60	2·24	28·0	10·14	1·21	21·9	9·34	12·8	4·85
19 00												
	—	—	68·9	21·02	2·42	35·7	12·88	1·63	27·4	10·90	14·4	5·45
	—	—	63·1	20·55	2·13	48·0	16·22	2·08	35·2	12·60	16·2	6·10
	59·5	18·91										
20 00	46·5	15·41	50·0	16·71	1·77	59·0	19·80	2·52	43·5	14·72	18·3	6·75
	37·7	12·93										
	30·4	10·85	35·5	12·54	1·20	64·3	20·72	2·83	48·6	16·00	20·4	7·40
	25·4	9·19										
	21·3	7·65	25·6	9·91	1·01	60·0	19·28	2·70	49·3	16·37	22·0	7·93
21 00	18·7	6·59										

TABLE II—*continued*

RA h m	$\delta = 00°$		$\delta = +16°$			$\delta = +40°$			$\delta = +50°$		$\delta = +65°$	
	T_{408}	T_{610}	T_{408}	T_{610}	T_{1407}	T_{408}	T_{610}	T_{1407}	T_{408}	T_{610}	T_{408}	T_{610}
	16·9	5·92	20·0	8·00	0·83	49·0	16·10	2·26	45·4	16·19	23·8	8·58
	14·8	5·42										
	13·6	4·81	16·8	6·57	0·67	37·2	13·32	1·84	40·3	15·52	26·4	9·11
	12·2	4·50										
22 00	11·4	3·88	14·3	5·61	0·57	28·6	10·97	1·53	33·4	14·30	29·2	9·64
	—	—	12·5	4·90	—	23·7	9·48	1·35	29·4	13·59	31·8	10·45
	—	—	11·0	4·48	—	21·0	8·26	1·24	27·6	13·15	33·9	10·89
23 00												
	—	—	9·7	—	—	19·0	7·92	1·10	25·9	12·84	35·3	11·48
	—	—	—	—	—	17·9	7·62	1·09	24·3	12·42	35·3	11·95
24 00	—	—	—	—	—	17·5	7·51	1·01	22·8	11·89	34·6	11·83

14 days'. The antenna temperature difference $(T_1 - T_2)$ measured when the axis of the observing antenna was directed at the celestial coordinates (α, δ) was converted to the mean sky brightness temperature $T(\alpha, \delta)$ by means of the formula

$$T(\alpha, \delta) = 0{\cdot}5[1 + 0{\cdot}008 \sec(\delta - \delta_0) + 0{\cdot}005](T_1 - T_2) + 0{\cdot}05 \cos 2\alpha$$

where $\delta_0 = +52°$ is the latitude of the observatory. The secant term is the correction for atmospheric attenuation (Howell 1968), the next term is the correction for antenna loss (Howell 1968), and the cosine term is the correction to the polar reference temperature for the fact that neither the antenna response pattern nor the brightness temperature distribution at the pole was circularly symmetrical. The correction was scaled from measurements of the semi-diurnal polar variation made by Howell (1968) with the 408 and 610 MHz antennas, using an assumed index $\beta = 2{\cdot}8$. The linear polarization temperatures at 1407 MHz measured by Bingham (1966) north of $\delta = +80°$ and averaged over the present beam size were too small to need inclusion in this term. The mean sky brightness temperatures at 1407 MHz are listed in Table II.

The daily records combined into the 1407 MHz drift scans were not all of the same length, so the signal-to-noise ratio near the beginning and end of each observed strip is not as good as that near the middle. The rms scatter on the average temperatures near the middle of the scans, as judged from the daily repeatability of the measurements, was 0·04 K at $\delta = +16°$ and 0·02 K at $+40°$.

Although all three experiments were designed to keep the zero levels of measurement constant, no attempt was made to determine the levels absolutely because the differential spectral index was deduced from the slopes of the T–T plots, which are independent of the positions of the origins of the plots. Thus the temperatures listed in Table II were measured with respect to undetermined zero levels. At all three frequencies, data obtained near midday were discarded in order to exclude the possibility of contamination by solar radiation.

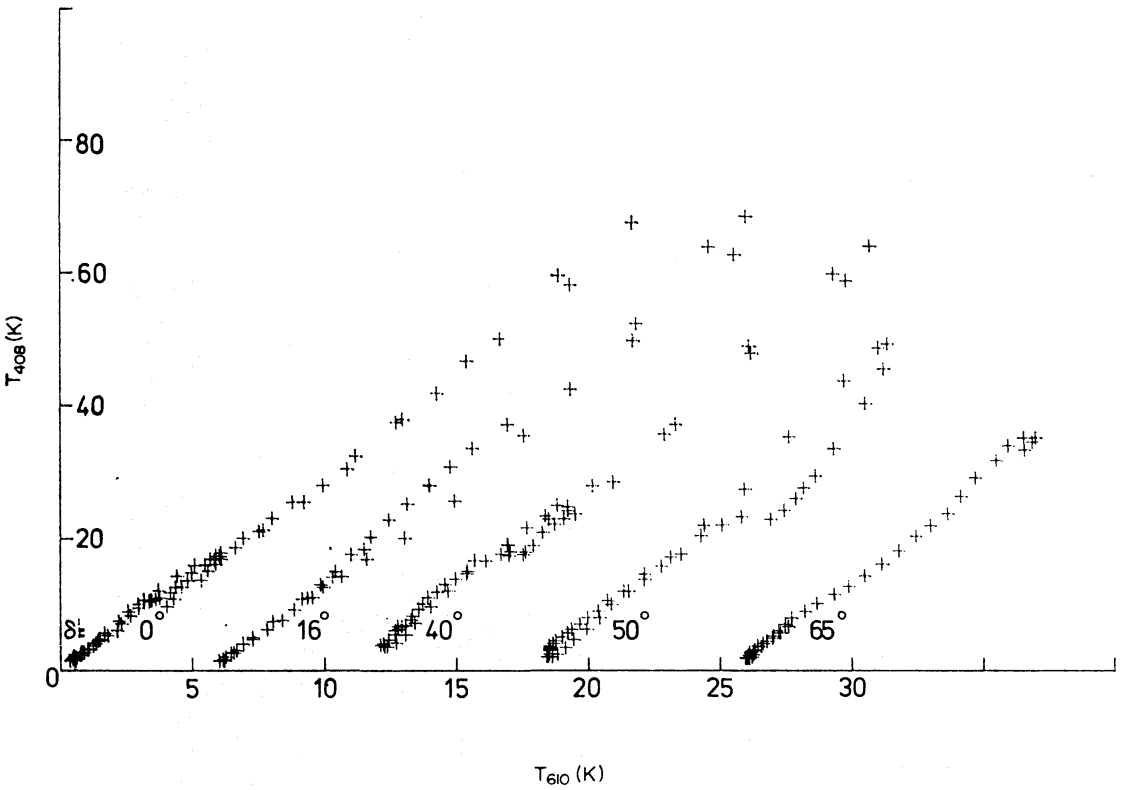

FIG. 3. *T–T plots between the* 408 *and* 610 *MHz mean sky brightness temperatures. The five individual plots are to the same scale, but their origins are unrelated.*

4. DERIVATION OF SPECTRAL INDICES

4.1 β *between* 408 *and* 610 *MHz*

Fig. 3 shows the T–T plots of the sky brightness temperatures for the five declination strips observed. The high-temperature parts of these plots, corresponding to the unresolved galactic plane, are unreliable because the strong gradients of sky brightness, coupled with the likely antenna pointing errors of about 1°, cause false spectral index variations. The index deduced for regions away from the plane is unaffected by this source of error on account of the smaller brightness gradients.

It is apparent that all five plots have similar mean slopes but that there are indications of systematic variations of slope for particular areas. In order to demonstrate this, Fig. 4 shows T–T plots between temperatures measured at positive galactic latitudes only. Separate plots are drawn at each declination for the zones preceding (A) and following (B) the points at each declination with the minimum measured temperatures. These zones correspond closely with Regions I and II of Bridle (1967), relating to 'spiral arm' and 'interarm' emission respectively. Data to which the unresolved galactic plane, the North Galactic Spur at $\delta = +16°$ and Loop IV near $\alpha = 13^h$, $\delta = 0°$ contributed appreciably have been excluded. The lines drawn on the plots were fitted by means of a least-squares programme. The values of $n = (dT_{408}/dT_{610})$ and its formal standard deviation $\sigma(n)$ calculated by the programme are listed in columns 5 and 6 of Table III. Column 7 contains the temperature differential indices β calculated from the relationship

$$n = \left(\frac{408}{610}\right)^{-\beta}.$$

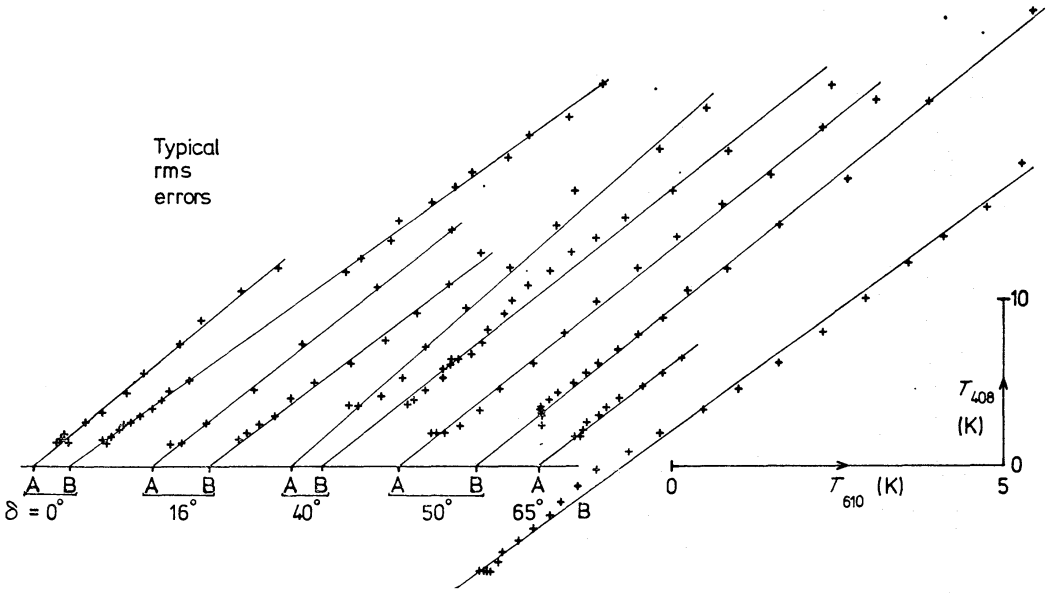

FIG. 4. *T–T plots between the 408 and 610 MHz mean sky brightness temperatures at positive galactic latitudes only. Each straight line is the least-squares fit to the data points in each plot.*

At each declination, *T–T* plots were also drawn containing the points from zones A and B taken together; corresponding values of n, $\sigma(n)$ and β are listed in the last three columns of Table III.

The mean values of the indices listed in columns 7 and 10 were calculated in two ways: first, weighted by the number of points in the *T–T* plot from which each index was derived and, secondly, unweighted. The weighted and unweighted mean indices in column 7 are 2·81 and 2·85, and in column 10, 2·77 and 2·77 respectively. The standard deviation of the ten indices in column 7 about the mean value 2·80 is 0·15, so the standard deviation of the mean may be inferred to be 0·05. This value is comparable with the scatter in the various weighted and unweighted means from columns 7 and 10 so it appears to be a good estimate of the error in the determination. It is concluded that the mean value of the differential index at high

TABLE III

The zones and the measured differential indices

Dec.	Zone	Range of RA h m h m	No. of pts	n $\sigma(n)$	β	n $\sigma(n)$	β
0°	A	07 18–09 42	12	3·30±0·06	2·97	2·85±0·04	2·60
	B	09 42–11 54 and 14 06–16 18	22	2·86±0·03	2·61		
+16°	A	07 24–09 48	7	3·16±0·05	2·86	3·06±0·05	2·79
	B	09 48–14 12	11	2·99±0·08	2·73		
+40°	A	05 48–10 12	11	3·54±0·09	3·14	3·29±0·08	2·96
	B	10 12–18 36	21	3·15±0·08	2·85		
+50°	A	05 00–11 00	15	3·18±0·05	2·87	3·16±0·06	2·86
	B	11 00–19 24	21	3·21±0·04	2·90		
+65°	A	07 00–11 48	11	3·00±0·01	2·73	2·91±0·03	2·65
	B	11 48–21 48	25	2·92±0·04	2·66		
1	2	3	4	5 6	7	8 9	10

northern latitudes is $\beta = 2{\cdot}80 \pm 0{\cdot}05$ between 408 and 610 MHz. No increase is necessary in the error estimate to account for the calibration error because the six calibrations at each frequency were separately included in different sections of the data, and therefore the scatter in the calibrations is implicitly included in the scatter in the calculated indices.

The value of 0·15 for the standard deviation of an index in column 7 is much greater than the value 0·02 or so which would be expected if the experimental spread of the temperature values in Table II were the only source of scatter in the values of the indices. This effect is almost certainly due to variations of the spectrum of the background radiation across the sky; it is too large to be the result either of drift in the receivers or of errors in pointing the antennas, and the systematic trends of the points about the lines have angular scales greater than a beamwidth. Landecker & Wielebinski (1969) found a similar systematic trend, with an angular scale of about 8°, on a T–T plot between temperatures from scaled antennas at 85 and 397 MHz; it was at a declination unobservable from Cambridge so it is not possible to say whether there is a corresponding feature between 408 and 610 MHz.

The unweighted mean of the five indices in column 7 of Table III from the zones labelled A is $2{\cdot}92 \pm 0{\cdot}07$, and from those labelled B is $2{\cdot}75 \pm 0{\cdot}06$; the weighted means agree with the unweighted to within 0·01. Therefore the mean index from the zones A is about two standard deviations greater than the grand average value of 2·80, and the mean from zones B is about one standard deviation smaller. The mean indices deduced by Bridle for Areas I and II differed in the opposite sense. However, the difference found in the present experiments is barely significant, and it is concluded that the differential indices between 408 and 610 MHz in the two regions are identical within the errors of measurement.

4.2 β *to* 1407 *MHz*

The 408/1407 and 610/1407 MHz T–T plots at $\delta = +16°$ are shown in Fig. 5. Division of the plot into two zones A and B defined as before gave the following indices and deviations:

	Zone A	Zone B
408/1407 MHz	$\beta = 2{\cdot}91 \pm 0{\cdot}12$	$2{\cdot}61 \pm 0{\cdot}05$
610/1407 MHz	$2{\cdot}97 \pm 0{\cdot}20$	$2{\cdot}56 \pm 0{\cdot}06$.

These values are poor estimates of the differential indices because the range of brightness temperatures is small at 1407 MHz and because the 1407 MHz temperatures come from one end of the RA coverage, where few days' data were combined into each average temperature.

To gain accuracy all the data points collected away from the unresolved plane were used. The lines fitted to these T–T plots gave the following values:

408/1407 MHz	$\beta = 2{\cdot}82 \pm 0{\cdot}03$
610/1407 MHz	$2{\cdot}77 \pm 0{\cdot}04$.

The errors in the line-fitting, the calibrations and the semi-diurnal polar correction may be combined to give about 0·05 for the rms error in these indices. It is probable, however, that this value is over-optimistic because the principal contribution is

from the formal error in the line-fitting; it is plain from the various estimates of index in column 7 of Table III that the small-scale variations in the index contribute a greater uncertainty, at least between 408 and 610 MHz, and it is likely that this effect is also present at higher frequencies. In consequence of this it is thought prudent to double the estimated error. Although the region of the North Galactic Spur was included with the general background for this analysis, the points affected by the radiation from this feature lay near the middle of the T–T plot and so the slope of the fitted line was unaffected by its steep spectrum (see Section 4.3). As will be shown below, the $\delta = +40°$ data at 1407 MHz were strongly influenced by an anomalous region of emission and could not be used to provide a measure of the general background index.

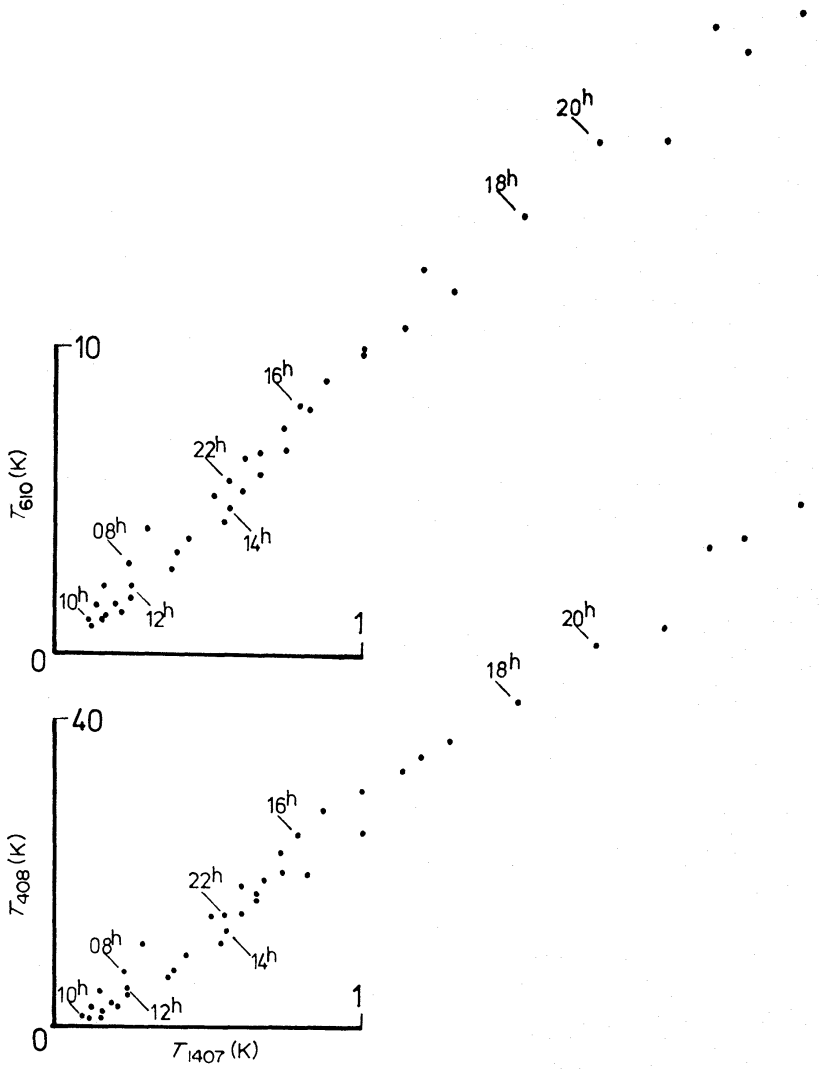

FIG. 5. 408/1407 *and* 610/1407 *MHz T–T plots on* $\delta = +16°$.

It is concluded that the best estimates of the spectral index of the background radiation are $2{\cdot}80 \pm 0{\cdot}05$ between 408 and 610 MHz, $2{\cdot}82 \pm 0{\cdot}1$ between 408 and 1407 MHz, and $2{\cdot}77 \pm 0{\cdot}1$ between 610 and 1407 MHz. These values are consistent with the value 2·80 between all three pairs of frequencies.

Some of the regions with anomalous spectra found on the T–T plots could be identified with known features of the continuum background. The very peculiar

region at about 13^h of RA on $\delta = 0°$ (Loop IV; Berkhuijsen, Haslam & Salter 1971) requires a full discussion which will be given separately, but the spectra of Loops I and III are dealt with here.

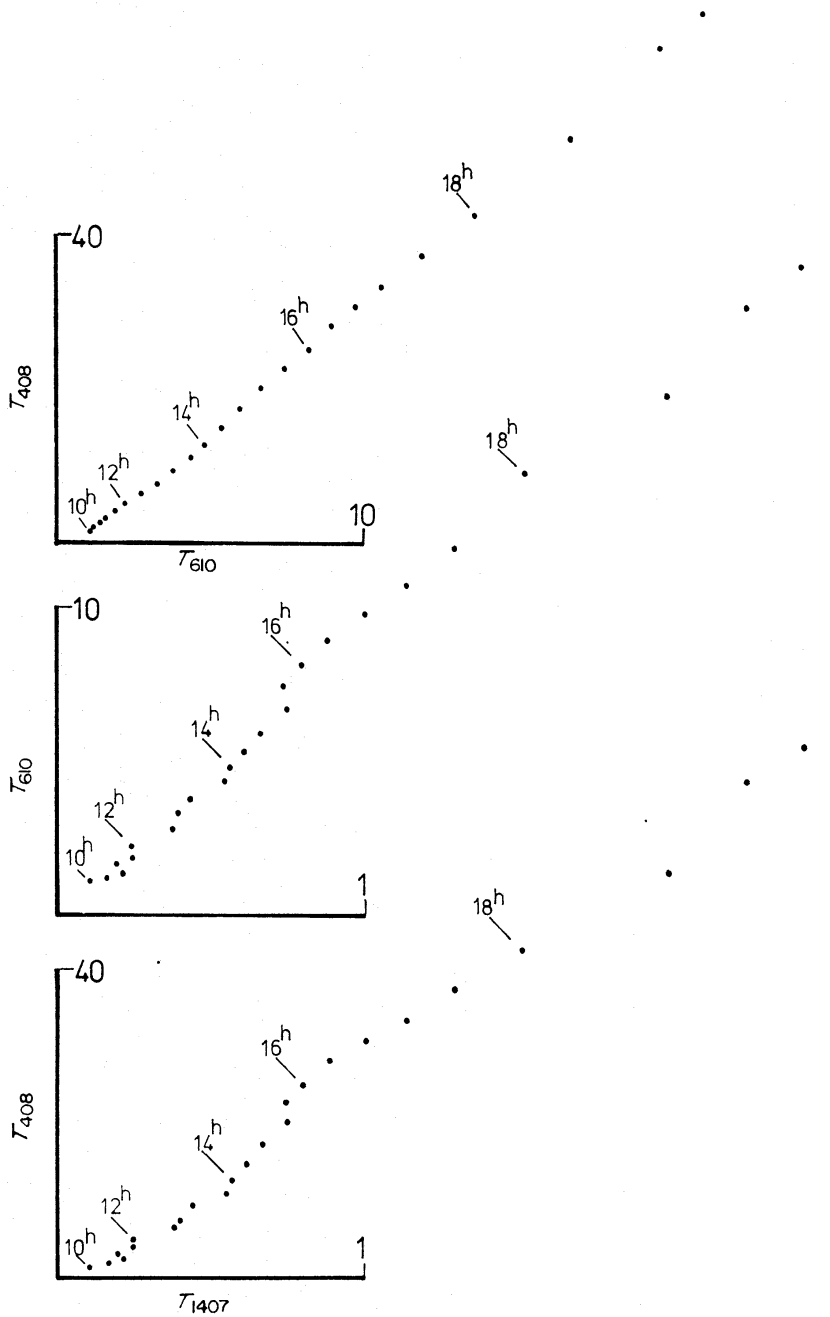

FIG. 6. *T–T plots between all three pairs of frequencies on* $\delta = +16°$, *between* 10^h *and* 20^h *of R.A., showing the effect of the Spur between* 14^h *and* 18^h. *The unit of brightness temperature is* 1 *K on both axes.*

4.3 *The spectrum of Loop I, the North Galactic Spur*

4.3.1 *Observations at* $\delta = +16°$. Fig. 6 shows the *T–T* plots between all three pairs of frequencies between about 10^h and 19^h of RA. On each, the points between 15^h and 17^h lie systematically above the run of the neighbouring points, indicating that the spectrum of the Spur is steeper than that of the general back-

ground radiation. The situation is, however, complicated by the fact that the radiation from the Spur is strongly linearly polarized, especially at high frequencies (Bingham 1966; Spoelstra 1971). Although there exists polarization at 408 and 610 MHz it is sufficiently weak and poorly oriented over the 15° beamwidth of the horns that the points on the 408/610 MHz plot need little correction. The 1407 MHz temperatures were corrected by averaging by eye over a 15° diameter area the polarization vectors on Bingham's 1407 MHz map, and calculating from the averages what the temperatures measured at several right ascensions would have been if the horn antennas had averaged the fluxes in orthogonal polarizations. The effect of this correction on the 408/1407 and 610/1407 MHz T–T plots was to move the points near 17^h a little towards the mean line of the plot, to leave the points near 16^h where they were and, most significantly, to move the points near 15^h well above the mean line. Thus the relatively steep spectrum of the Spur at frequencies above 408 MHz is well established. Unfortunately it is difficult to say by how much the spectrum in this region is steeper than the galactic average.

4.3.2 *The observations at* $\delta = +40°$. The T–T plots between all three pairs of frequencies are shown in Fig. 7. Between 14^h and 18^h the slopes of the 408/1407 and 610/1407 MHz plots are very steep, and all three plots are strongly curved in the same sense in this region. This curvature corresponds to one of the clearest of the small-scale index fluctuations seen in Fig. 4. There is independent evidence of a spectral anomaly in this region:

(i) Berkhuijsen (1971) noted on her T–T plots of 240 and 820 MHz cuts through the Spur at constant galactic latitude that there was a change of spectrum across the ridge. Points on the north side had smaller 820 MHz brightness temperatures than points on the south side with the same 240 MHz temperatures;

(ii) Conklin's (1970) dual-beam 8 GHz experiment at $\delta = +32°$, performed to detect any large-scale anisotropy of the microwave background radiation, showed a marked effect at 16^h after correction for the galactic radiation. The residuals there swung from a large positive value to a large negative value; the sense of the swing was that which would be expected if the galactic correction, made by extrapolating the temperatures on a 404 MHz map (Pauliny-Toth & Shakeshaft 1962) to 8 GHz assuming a constant spectral index of 2·8, was overestimated near 16^h. This is clear evidence that the spectral index from 0·4 to 8 GHz is locally greater than the average. The 408 MHz temperatures near 16^h–17^h on the 408/1407 MHz plot show an excess of about 7 K over the line of best fit to the rest of the plot. If it is assumed that the feature has such a steep spectrum that it contributes nothing to the brightness temperatures measured at 1407 MHz and higher frequencies, the effect expected from the galactic correction in Conklin's residuals is $7 \times (0{\cdot}4/8)^{2{\cdot}8}$ K = 1·5 mK. The actual effect found by Conklin is about twice as large as this, which, in view of the simple assumption made here about the spectrum of the feature and the somewhat different declinations of the observations, is good agreement. It is clearly dangerous to draw conclusions about the anisotropy without making allowance for spectral anomalies of this sort.

Although $\delta = +40°$ is well to the north of the bright ridge of the Spur, it seems very likely that the anomalous region there is associated with the Spur. Berkhuijsen's result concerning the variation of spectral index across the ridge is evidence of this and there is also evidence from radio polarization surveys. The

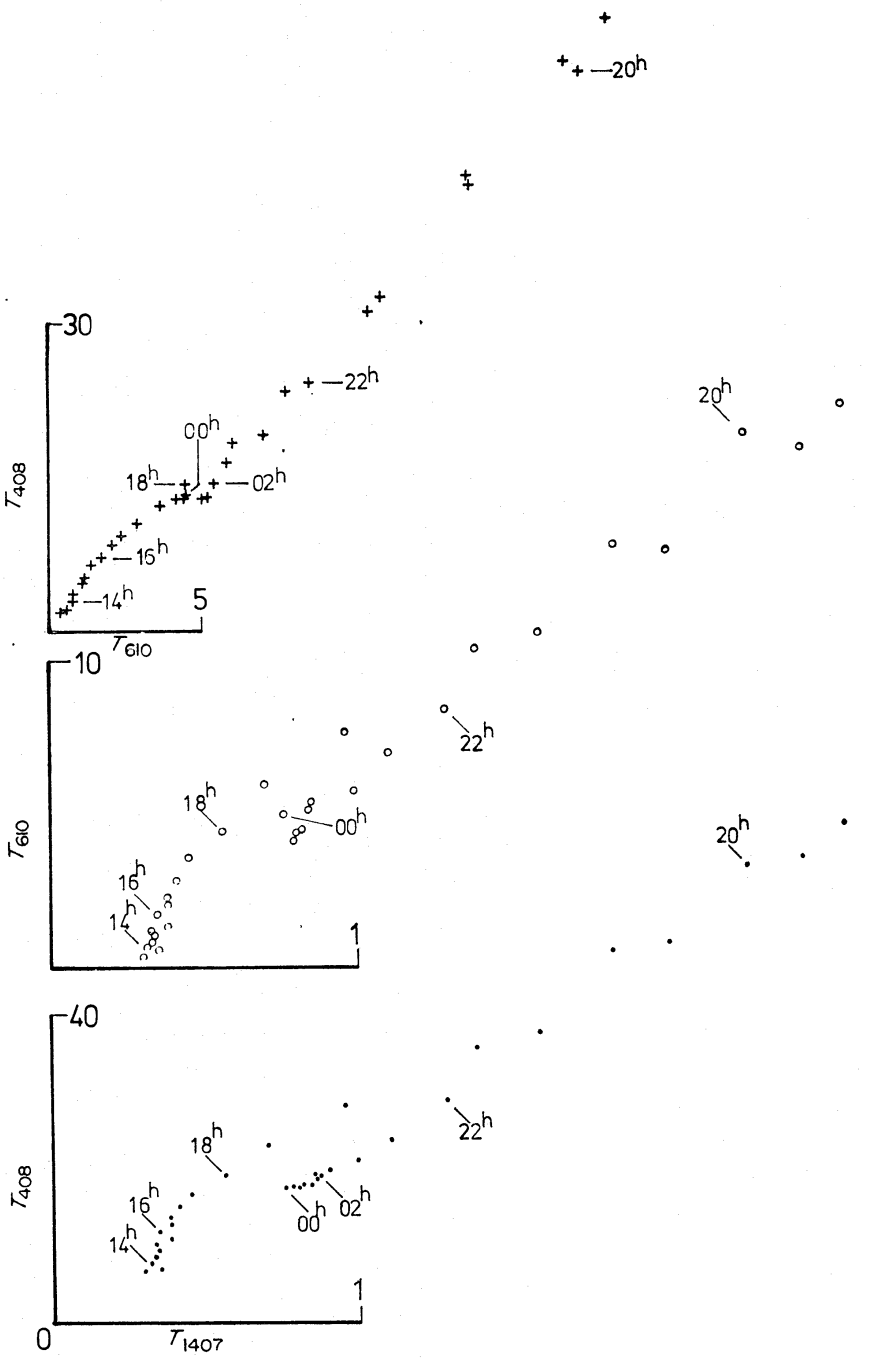

FIG. 7. *T–T plots between all three pairs of frequencies on* $\delta = +40°$. *The unit of brightness temperature is* 1 *K on both axes.*

polarization vectors at $\delta = +40°$ on the 1407 MHz map of Bingham (1966), for example, are small but systematically aligned; the alignment is a smooth continuation of the alignment of the vectors in the Spur proper. The alignment is lost by $\delta = +50°$, and its is significant that the present T–T plot at this declination shows no anomaly.

4.3.3 *The observations at* $\delta = 0°$. The alignment of the polarization vectors on Bingham's map shows that some of the radiation between 14^h and 16^h is associated with the Spur. However, there is no steepening discernible on the T–T plot B at

$\delta = 0°$; on the contrary the differential index of this plot is 2·61 which is smaller than the average. This is further confirmation of Berkhuijsen's result that the spectrum south of the ridge of the Spur is flatter than that to the north.

4.4 *The spectrum of Loop III*

At $\delta = +65°$ the antenna beams crossed the ridge of the continuum feature known as Loop III (Berkhuijsen *et al.* 1971) at RA $\approx 17^h\,05^m$. The points in this region of the 408/610 MHz T–T plot indicate the presence of a component with a spectrum locally steeper than the average. The slope of the line fitted to T–T plot B at $\delta = +65°$ gives $\beta = 2{\cdot}66$, however, *smaller* than the average value. This suggests that the inside of Loop III, that is the portion later than 17^h, has a spectrum flatter than the galactic spectrum.

Howell (1968) also found that the spectrum between 81·5 and 610 MHz within this Loop was flatter than the average. Thus Loop III resembles closely Loop I in the distribution of the spectral index.

4.5 *Discussion of the spectra of Loops I and III*

Previous spectral data for the ridge of the Spur have been reviewed by Holden (1967). Below about 30 MHz the spectrum appears to turn over to a negative value of the index, whilst above this frequency the index increases steadily. The steep spectrum above 408 MHz found in the present study confirms this trend.

If the emission from Loop I is synchrotron radiation, as is generally accepted, it is now possible to conclude that the electrons radiating in the Spur cannot have the same energy spectrum as those giving rise to the background, whatever assumption is made regarding the ratio of magnetic field strengths, because the radio spectra are so different.

It has already been proposed that Loops I and III are similar objects on account of their shapes and the association of H I with both (see e.g. Berkhuijsen *et al.* 1971). The similarity of the continuum spectrum variations found here gives further support to this proposition; the ridges of both Loops have spectra steeper than the average between 408 and 610 MHz and the regions inside the arcs of the Loops have spectra flatter than the average.

It is not clear at present how to apply these results to the problem of the origin of the Loops since none of the current hypotheses, e.g. the super-supernova remnant (Bingham 1967; Berkhuijsen *et al.* 1971) or the fossil Strömgren sphere (Brandt & Maran 1972), is sufficiently well developed for a reliable prediction of the radio spectrum of any part of the features to be made.

5. CONCLUSIONS

The scaled-horn experiments at 408, 610 and 1407 MHz show that the mean differential temperature spectral index at high northern galactic latitudes is close to the value $\beta = 2{\cdot}80$ between all three pairs of frequencies. The accuracy with which the index could be determined was limited ultimately by small variations of the index with direction and not by any instrumental effect. The clearest of the variations were identified with the continuum Loops I, III and IV. The regions of anomalous spectra associated with Loops I and III appear to extend some distance from the ridges of these features. The spectrum of the inside of each

ridge is a little flatter than the average for the Galaxy, and of the ridge itself considerably steeper; a region outside Loop I was also found to have a steep spectrum.

The correction for galactic emission made by Conklin to his 8 GHz measurements of background anisotropy was in error because of the region with anomalous spectrum just to the north of the Spur. It seems wisest that future anisotropy experiments be made at frequencies of 30 GHz or higher in order to render such a correction entirely negligible.

Mullard Radio Astronomy Observatory, Cavendish Laboratory, Cambridge

REFERENCES

Altenhoff, W., 1968. *Interstellar ionized hydrogen*, p. 519, ed. Y. Terzian, W. A. Benjamin.
Berkhuijsen, E. M., 1971. *Astr. Astrophys.*, **14,** 359.
Berkhuijsen, E. M., Haslam, C. G. & Salter, C. J., 1971. *Astr. Astrophys.*, **14,** 252.
Bingham, R. G., 1966. *Mon. Not. R. astr. Soc.*, **134,** 327.
Bingham, R. G., 1967. *Mon. Not. R. astr. Soc.*, **137,** 157.
Brandt, J. C. & Maran, S. P., 1972. *Nature*, **235,** 38.
Bridle, A. H., 1967. *Mon. Not. R. astr. Soc.*, **136,** 219.
Conklin, E. K., 1970. Ph.D. thesis, Stanford University.
Holden, D. J., 1967. Ph.D. thesis, University of Cambridge.
Howell, T. F., 1968. Ph.D. thesis, University of Cambridge.
Howell, T. F., 1970. *Astrophys. Lett.*, **6,** 45.
Landecker, T. L. & Wielebinski, R., 1969. *Proc. astr. Soc. Austr.*, **1,** 210.
Pauliny-Toth, I. I. K. & Shakeshaft, J. R., 1962. *Mon. Not. R. astr. Soc.*, **124,** 61.
Penzias, A. A. & Wilson, R. W., 1966. *Astrophys. J.*, **146,** 666.
Sironi, G., 1974. *Mon. Not. R. astr. Soc.*, **166,** 345.
Spoelstra, T. A. Th., 1971. *Astr. Astrophys.*, **13,** 237.
Webster, A. S., 1972. *J. Phys. E., Sci. Instr.*, **5,** 202.